Appl Phys B (2011) 104:1007–1012
DOI 10.1007/s00340-011-4521-4

Applied Physics B
Lasers and Optics

Average spreading of a linear Gaussian–Schell model beam array in non-Kolmogorov turbulence

H. Tang · B. Ou

Received: 12 November 2010 / Revised version: 24 January 2011 / Published online: 15 May 2011

Abstract The average spreading of a linear Gaussian–Schell model (GSM) beam array in non-Kolmogorov turbulence is studied, where the coherent combination is considered. The effects of the beam number, the separation distance between two adjacent beams and the generalized exponent on the root-mean-square (rms) beam width are investigated. The results indicate that the rms beam width in non-Kolmogorov turbulence is different from that in Kolmogorov turbulence, and there is an optimum beam number that leads to a minimum beam width. Further, the beam width can reach the minimum value by adopting the optimum separation distance, which decreases with the increase of beam number. Besides, the partially coherent beam array is less sensitive to the atmospheric turbulence than the fully coherent one.

1 Introduction

The optical propagation through the turbulent atmosphere is a very important subject in the case of the remote sensing, imaging and communication systems and has attracted considerable interests in the past decades. For a long time, the Kolmogorov model has been widely used to study the effects of the atmospheric turbulence on the free-space optical propagation. However, another type of turbulence as widespread as Kolmogorov turbulence is helical turbulence [1]. In the presence of the helical turbulence, the spectral properties of passive scalar field are changed. Moreover, recent experimental results also indicated great deviations from the predictions of the Kolmogorov model in some portions of the atmosphere [2–5]. The reason is that when the atmosphere is extremely stable, the turbulence is no longer homogeneous in three dimensions since the vertical component is suppressed, that is to say, in this case the turbulence is anisotropic [6]. And the anisotropic turbulence in the stratosphere has been experimentally investigated [7, 8]. Also, investigations have indicated that the turbulence in the shear layer created in laboratory is anisotropic. However, the properties of the turbulence in the tropopause are similar to that in the shear layer. And the experimental results also indicated that the Kolmogorov model cannot completely describe the turbulence near the tropopause [9]. Besides, the mechanisms of turbulent generation and dissipation are different at high and low altitudes, which results in the difference in turbulent spectrum [10]. In addition, the Kolmogorov model is valid only in the inertial subrange.

Thus, it is very important to find other models, which are more general than the Kolmogorov model to describe non-Kolmogorov turbulence. Then, a non-Kolmogorov model is presented [11, 12], which reduces to the Kolmogorov model only for the generalized exponent $\alpha = 3.67$. Using the non-Kolmogorov spectrum, the scintillation index, the signal-to-noise ratio (SNR) and the bit-error rate (BER) are studied [13]. As is known, spatial partially coherent beams are less affected by the atmospheric turbulence than the fully coherent beams [14]. And the average spreading of the GSM beam propagating in non-Kolmogorov turbulence is investigated [15]. Whereas in practice the laser beam array is widely used in many fields, such as the high-power system and the inertial confinement fusion. In addition, the average spreading of the linear Gaussian beam array propagating in Kolmogorov turbulence and non-Kolmogorov turbulence are studied [16, 17], respectively. Therefore, quantitative es-

H. Tang (✉) · B. Ou
School of Electronic and Information Engineering, Beihang University, Beijing 100191, China
e-mail: huatang@buaa.edu.cn

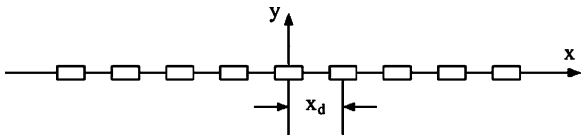

Fig. 1 Schematic diagram of the linear GSM beam array

timations of the average spreading of the partially coherent beam array through non-Kolmogorov turbulent atmosphere are necessary. Besides, the study of this subject has potential applications in improving the communication system performance in the real atmosphere.

In this paper, the beam spreading of a linear GSM beam array in non-Kolmogorov turbulence is investigated by using the rms beam width. The theoretical results show that the beam number and the generalized exponent have great effects on the beam width. Further, the beam width can reach the minimum value by adopting the optimum separation distance, which decreases with the increase of beam number.

2 Analytical formulas

Assume a linear GSM beam array composed of N equal beams is located in the plane $z=0$ with the separation distance between two adjacent beams x_d, as depicted in Fig. 1. For simplicity, the formulas obtained below are for odd N. For even N, the formulas are valid by changing the range of m and n into $1-N/2$ to $N/2$. For the coherent combination, the cross-spectral density function of the linear GSM beam array for odd N is defined as [18]

$$w^0(x_1,x_2,z=0) = \sum_{m=-(N-1)/2}^{(N-1)/2}\sum_{n=-(N-1)/2}^{(N-1)/2}\exp\left(-\frac{(x_1-mx_d)^2+(x_2-nx_d)^2}{w_0^2}\right) \times \exp\left(-\frac{[(x_1-mx_d)-(x_2-nx_d)]^2}{2\sigma_0^2}\right), \tag{1}$$

where w_0 and σ_0 are the waist width and the coherent width of the GSM beam. Based on the extended Huygens–Fresnel principle, the average intensity of the linear GSM beam array propagating through non-Kolmogorov turbulent atmosphere at the receiving plane is expressed as [17]

$$\langle I(x,z)\rangle = \frac{1}{\lambda z}\int_{-\infty}^{\infty}\int_{-\infty}^{\infty} w^0(x_1,x_2,z=0) \times \exp\left\{\frac{ik}{2z}\left[\left(x_1^2-x_2^2\right)-2x(x_1-x_2)\right]\right\} \times \left\langle\exp\left[\psi^*(x,x_1,z)+\psi(x,x_2,z)\right]\right\rangle dx_1\,dx_2, \tag{2}$$

where the term $\langle\exp[\psi^*(x,x_1,z)+\psi(x,x_2,z)]\rangle$ is given by [17]

$$\left\langle\exp\left[\psi^*(x,x_1,z)+\psi(x,x_2,z)\right]\right\rangle = \exp\left\{-4\pi^2\kappa^2 z\int_0^1\int_0^{\infty}\kappa\phi_n(\kappa,\alpha) \times\left[1-J_0\left(\kappa\xi|x_1-x_2|\right)\right]d\kappa\,d\xi\right\},$$

in which k is the wave number, κ is the magnitude of two-dimensional spatial frequency and J_0 is the Bessel function of the first kind and zero order.

The rms beam width of the linear GSM beam array propagating in non-Kolmogorov turbulence is defined as [17]

$$w = \left[4\int_{-\infty}^{\infty}x^2\langle I(x,z)\rangle dx \Big/ \int_{-\infty}^{\infty}\langle I(x,z)\rangle dx\right]^{1/2}. \tag{3}$$

Upon substituting (2) into (3), and using the integral transform technique, after tedious integral calculations, as shown in Appendix, we obtain

$$w = \left(A+Bz^2/k^2+8/3Tz^3\right)^{1/2}, \tag{4}$$

where

$$A = \frac{\sum_{m=-(N-1)/2}^{(N-1)/2}\sum_{n=-(N-1)/2}^{(N-1)/2}\exp\left[-\left(\frac{1}{2w_0^2}+\frac{1}{2\sigma_0^2}\right)(m-n)^2x_d^2\right]\left[w_0^2+(m+n)^2x_d^2\right]}{\sum_{m=-(N-1)/2}^{(N-1)/2}\sum_{n=-(N-1)/2}^{(N-1)/2}\exp\left[-\left(\frac{1}{2w_0^2}+\frac{1}{2\sigma_0^2}\right)(m-n)^2x_d^2\right]},$$

$$B = \frac{\sum_{m=-(N-1)/2}^{(N-1)/2}\sum_{n=-(N-1)/2}^{(N-1)/2}4\left(\frac{1}{w_0^2}+\frac{1}{\sigma_0^2}\right)\exp\left[-\left(\frac{1}{2w_0^2}+\frac{1}{2\sigma_0^2}\right)(m-n)^2x_d^2\right]\left[1-\left(\frac{1}{w_0^2}+\frac{1}{\sigma_0^2}\right)(m-n)^2x_d^2\right]}{\sum_{m=-(N-1)/2}^{(N-1)/2}\sum_{n=-(N-1)/2}^{(N-1)/2}\exp\left[-\left(\frac{1}{2w_0^2}+\frac{1}{2\sigma_0^2}\right)(m-n)^2x_d^2\right]},$$

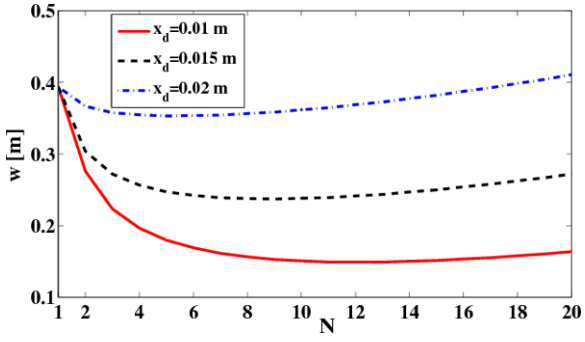

Fig. 2 The rms beam width w as a function of N with $z = 10$ km, $\tilde{C}_n^2 = 1 \times 10^{-15}$ m$^{3-\alpha}$, $\alpha = 3.8$, $\sigma_0 = 0.01$ m and $x_d = 0.015$ m

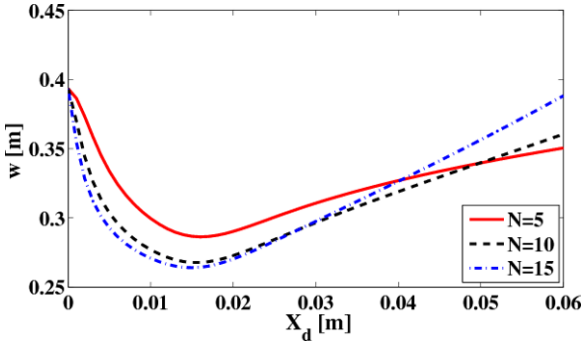

Fig. 3 w as a function of x_d for different N with $z = 10$ km, $\tilde{C}_n^2 = 1 \times 10^{-15}$ m$^{3-\alpha}$, $\alpha = 3.8$ and $\sigma_0 = 0.01$ m

and

$$\mathrm{T} = \pi^2 \int_0^\infty \kappa^3 \phi_n(\kappa, \alpha)\, d\kappa.$$

Considering the inner-scale and outer-scale effects, the non-Kolmogorov spectrum is defined as [19]

$$\phi_n(\kappa, \alpha) = A(\alpha)\tilde{C}_n^2 \cdot \exp\left(-\kappa^2/\kappa_m^2\right) \cdot \left(\kappa^2 + \kappa_0^2\right)^{-\alpha/2},$$
$$0 \le \kappa < \infty, \quad 3 < \alpha < 4, \tag{5}$$

where $A(\alpha) = \Gamma(\alpha - 1) \cdot \cos(\alpha\pi/2)/(4\pi^2)$, $\kappa_0 = 2\pi/L_0$ and $\kappa_m = c(\alpha)/l_0$, in which $c(\alpha) = \{\Gamma[(5-\alpha)/2] \cdot A(\alpha) \cdot 2\pi/3\}^{1/(\alpha-5)}$, l_0 is the inner scale and L_0 is the outer scale. Using the non-Kolmogorov spectrum, after some tedious mathematical manipulation, the term T is expressed as [15]

$$\mathrm{T} = \pi^2 A(\alpha)\tilde{C}_n^2 \big/ \left[2(\alpha - 2)\right] \cdot \left[\kappa_m^{2-\alpha}\left(2\kappa_0^2 - 2\kappa_m^2 + \alpha\kappa_m^2\right)\right.$$
$$\left. \times \exp\left(\kappa_0^2/\kappa_m^2\right) \cdot \Gamma\left(2 - \alpha/2, \kappa_0^2/\kappa_m^2\right) - 2\kappa_0^{4-\alpha}\right],$$

where Γ denotes the Gamma function.

3 Analysis and results

In numerical simulations, for simplicity, we choose $\lambda = 850$ nm, $w_0 = 0.01$ m, $L_0 = 1$ m and $l_0 = 0.01$ m. With typical parameters, $z = 10$ km, $\tilde{C}_n^2 = 1 \times 10^{-15}$ m$^{3-\alpha}$, $\alpha = 3.8$, $\sigma_0 = 0.01$ m and $x_d = 0.015$ m, the influences of N on the rms beam width for different x_d are depicted in Fig. 2. It shows that there is an optimum N that leads to a minimum rms beam width and the optimum N decreases with the increase of x_d. The existence of the optimum N can be understood as follows. For given x_d, when N is relatively small, the beams of the beam array interfere with each other, which leads to a smaller rms beam width w, compared with $N = 1$. However, when N is large enough, some beams may become independent of each other, which results in a larger w. The variation of w with x_d for different N is shown in Fig. 3.

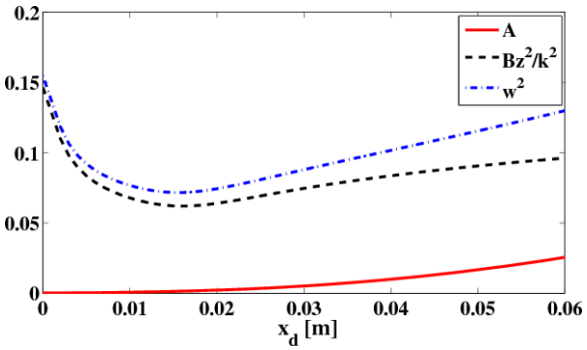

Fig. 4 A, Bz^2/k^2 and w^2 as a function of x_d with $z = 10$ km, $\tilde{C}_n^2 = 1 \times 10^{-15}$ m$^{3-\alpha}$, $\alpha = 3.8$, $\sigma_0 = 0.01$ m and $N = 10$

For multiple beams ($N \ge 2$), there is an optimum separation distance x_{dm} which leads to a minimum w and this x_{dm} depends strongly on N.

In this paper, we concentrate on the discussion of the optimum separation distance for the reason that it is more controllable than the beam number in the experiments, especially for lasers with high power. The existence of the optimum separation distance is investigated analytically and physically. The three terms in the bracket on the right-hand side of (4) denote the equivalent beam width of the linear GMS beam array at $z = 0$, the diffractive spreading of the beam array in free space and the spreading resulting from the atmospheric turbulence, respectively. The first term A is a monotonically increasing function of x_d and the second term Bz^2/k^2 is not a monotone function of x_d. Further, the atmospheric part (the third term) is independent of x_d, so that the x_{dm} has no relation with the atmospheric parameters $\tilde{C}_n^2$ and α, which can be demonstrated by (4). Therefore, it is not necessary to consider the effects of the atmospheric parameters on x_{dm} for designing the optical communication system.

A, Bz^2/k^2 and w^2 as a function of x_d with $N = 10$ are plotted in Fig. 4. The result shows that the optimum separation distance x_{dm} results from the second term in the bracket on the right-hand side of (4). Therefore, when the second

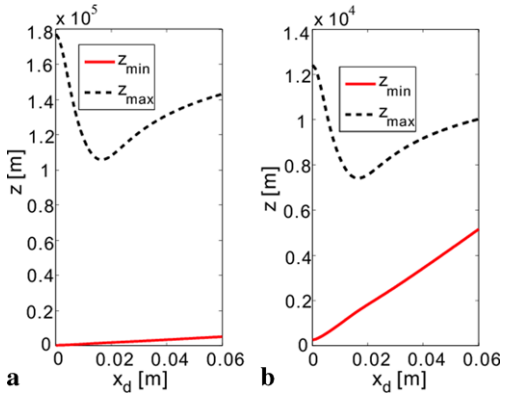

Fig. 5 $z_{\max}$ and $z_{\min}$ as a function of x_d with $\sigma_0 = 0.01$ m and $N = 10$, (**a**) $\tilde{C}_n^2 = 1 \times 10^{-15}$ m$^{3-\alpha}$, $\alpha = 3.8$ and (**b**) $\tilde{C}_n^2 = 1 \times 10^{-14}$ m$^{3-\alpha}$, $\alpha = 3.67$

term Bz^2/k^2 is relatively larger than the first term A and the third term $8/3Tz^3$, the optimizing effect of x_d will be rather obvious, otherwise the optimization may still exist but not obvious enough. In order to achieve the better optimizing effect, the effective range of z can be obtained by $Bz^2/k^2 > A$ and $Bz^2/k^2 > 8/3Tz^3$. Based on the analysis above, the effective range of z is expressed as

$$z_{\min} = \sqrt{A/B} \cdot k < z < 3B/\left(8Tk^2\right) = z_{\max}. \tag{6}$$

Equation (6) indicates that when the propagation distance z is in the effective range of $z_{\min}$ to $z_{\max}$, the optimizing effect of x_d on the rms beam width will be rather obvious. The effective range of z as a function of x_d is plotted in Fig. 5(a). It can be seen that $z = 10$ km is in the effective range of $z_{\min}$ to $z_{\max}$ for $x_d = 0.015$ m, and so the optimizing effect of x_d is rather obvious, which is the reason for choosing $z = 10$ km in our simulations.

A physical understanding of the existence of x_{dm} is that when x_d is relatively small, the interference of the beams with each other makes the intensity of the beam array more focused and a smaller w is obtained. When x_d is too large, some beams may become independent of each other and a larger w is obtained. For $x_d = 0$, the beams overlap with each other, i.e., the beam array is equal to a single beam, and then the cases with different N have the equal rms beam widths, as shown in Fig. 3. The dependence of the optimum separation distance x_{dm} on N is also manifested in Fig. 3. The specific relation between x_{dm} and N is shown in Fig. 6, which indicates that x_{dm} decreases with the increase of N.

The analysis above only consider the case of $\alpha = 3.8$. However, the generalized exponent α is variable as the linear GSM beam array propagates through non-Kolmogorov turbulent atmosphere. Next, the effects of $\tilde{C}_n^2$ and α are studied. As shown in Fig. 7, when α is smaller than 3.67 and not close to 3, there is a larger w compared with $\alpha = 3.67$ and when α is close to 3, w decreases rapidly since in this case,

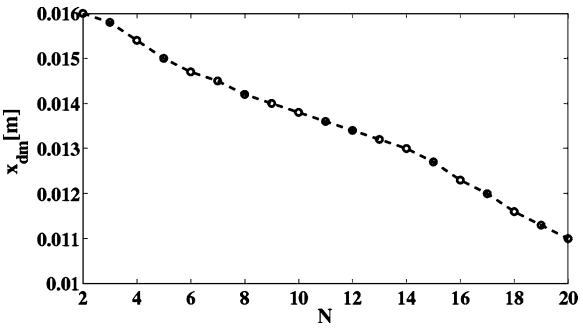

Fig. 6 The optimum separation distance x_{dm} as a function of N with $z = 10$ km, $\tilde{C}_n^2 = 1 \times 10^{-15}$ m$^{3-\alpha}$, $\sigma_0 = 0.01$ m and $\alpha = 3.8$

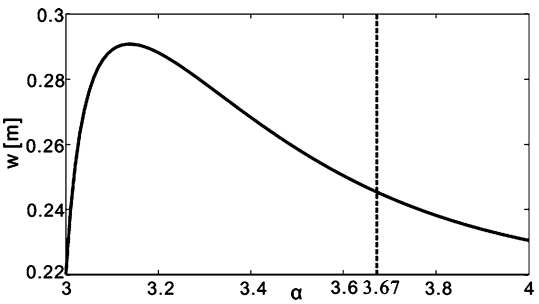

Fig. 7 w as a function of α with $z = 10$ km, $\tilde{C}_n^2 = 1 \times 10^{-15}$ m$^{3-\alpha}$, $\sigma_0 = 0.01$ m, $N = 10$ and $x_d = 0.015$ m

$A(\alpha)$ begins to decrease to zero. Besides, when α is larger than 3.67, there is a smaller w.

Although the optimum separation distance x_{dm} is independent of $\tilde{C}_n^2$ and α, the optimizing effect of x_d has great dependence on $\tilde{C}_n^2$ and α. It can be understood by that with the increase of $\tilde{C}_n^2$ and the variation of α, $z = 10$ km may be not in the effective range of $z_{\min}$ to $z_{\max}$, which can be demonstrated by (6). When $\tilde{C}_n^2 = 1 \times 10^{-14}$ m$^{3-\alpha}$, $\alpha = 3.67$, $N = 10$ and $x_d = 0.015$ m, $z = 10$ km is not in the effective range of $z_{\min}$ to $z_{\max}$, as shown in Fig. 5(b). In this case, the optimizing effect of x_d will be weakened, as shown in Fig. 8.

We know that the partially coherent beams are less affected by the turbulence than the fully coherent ones. Thus, an interesting question arises: does the result hold true for the partially coherent beam array? Figure 9 plots the rms beam width w as a function of the propagation distance z for different $\tilde{C}_n^2$ and σ_0. Through comparing the differences between w in the turbulence and that in free space ($\tilde{C}_n^2 = 0$) for $\sigma_0 = 0.01$ m and $\sigma_0 = \infty$, it can be indicated that the partially coherent beam array is also less sensitive to the turbulence than the fully coherent one, especially for the long-distance communication. Further, the influence of the turbulence on w increases with increasing z. It can be understood by that the influence of the turbulence on the beam array propagation accumulates along the propagation path.

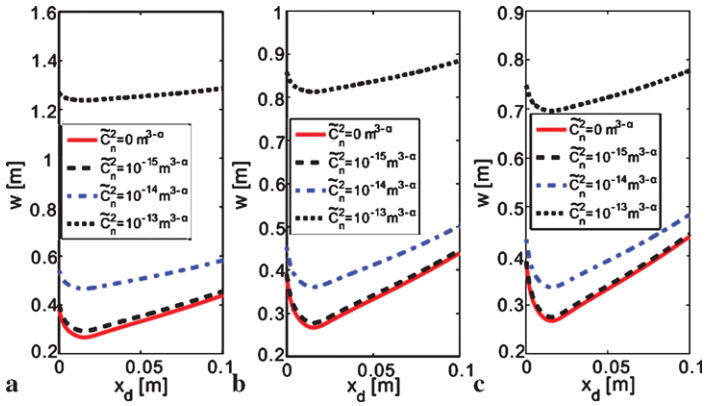

Fig. 8 w as a function of x_d for different $\tilde{C}_n^2$ with $z = 10$ km, $\sigma_0 = 0.01$ m, $N = 10$, (**a**) $\alpha = 3.3$, (**b**) $\alpha = 3.67$ and (**c**) $\alpha = 3.8$

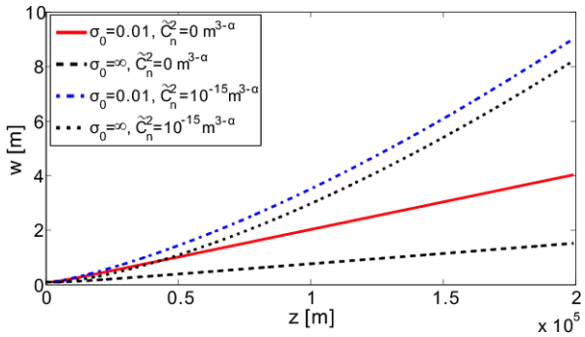

Fig. 9 w as a function of the propagation distance z for different $\tilde{C}_n^2$ and σ_0 with $\alpha = 3.8$, $N = 10$ and $x_d = 0.015$ m

4 Conclusions

In summary, the effects of the beam number N, the generalized exponent α and the separation distance x_d on the rms beam width of the linear Gaussian beam array propagating in non-Kolmogorov turbulence are investigated. The theoretical results indicate that the rms beam width in non-Kolmogorov turbulence is different from that in Kolmogorov turbulence with $\alpha = 3.67$, and there is an optimum beam number that leads to a minimum w. Further, the beam width can reach the minimum value by adopting the optimum separation distance, which decreases with the increase of beam number. Besides, the optimizing effect of x_d on the rms beam width has great dependence on $\tilde{C}_n^2$ and α, which manifests that the spreading and focusing ability of the linear GSM beam array propagating in non-Kolmogorov turbulence is so different from that in Kolmogorov turbulence that a specific treatment is required when non-Kolmogorov turbulence exists. Therefore, the non-Kolmogorov spectrum should be considered in real system optimization. In addition, the partially coherent beam array is less sensitive to the atmospheric turbulence than the fully coherent beam array.

Acknowledgements This work is supported by the Key Project of National Natural Science Foundation of China (Grant No. 60837004), the Project-sponsored by SRF for ROCS, SEM, Fundamental Research Funds for the Central Universities (Grant No. YWF-10-02-031), the innovation Foundation of CAST (Grant No. 20090304), and the National Hi-Tech Research and Development (863) Program.

Appendix: Derivation of (4)

With the new integral variables $u = (x_1 + x_2)/2$, $v = x_2 - x_1$, (2) can be rewritten as

$$\begin{aligned}\langle I(x,y,z)\rangle = \frac{k}{2\pi z}\sum_{m=-(N-1)/2}^{(N-1)/2}\sum_{n=-(N-1)/2}^{(N-1)/2}\int_{-\infty}^{\infty}\int_{-\infty}^{\infty}\exp\left[\frac{ik}{z}(xv-uv)\right]du\,dv \\ \times\exp\left[-\frac{2u^2+v^2/2-2(m+n)x_d u+(m-n)x_d v+(m^2+n^2)x_d^2}{w_0^2}\right] \\ \times\exp\left[-\frac{v^2+2(m-n)x_d v+(m-n)^2x_d^2}{2\sigma_0^2}\right]\exp\left\{-4\pi^2k^2z\int_0^1\int_0^{\infty}\kappa\phi_n(\kappa,\alpha)\left[1-J_0(\kappa\xi v)\right]d\kappa\,d\xi\right\}. \quad (A.1)\end{aligned}$$

Equation (3) can be written as

$$w = (F_1/F_2)^{1/2}, \quad (A.2)$$

where

$$F_1 = 4\int_{-\infty}^{\infty} x^2 \langle I(x,z)\rangle dx, \tag{A.3}$$

$$F_2 = \int_{-\infty}^{\infty} \langle I(x,z)\rangle dx. \tag{A.4}$$

Upon substituting (A.1) into (A.3) and recalling the integral formula $\int_{-\infty}^{\infty} x^2 \exp(i\mu x s)\,dx = -2\pi/\mu^3 \delta''(s)$, we obtain

$$\begin{aligned} F_1 = {} & -4\left(\frac{z}{k}\right)^2 \sum_{m=-(N-1)/2}^{(N-1)/2} \sum_{n=-(N-1)/2}^{(N-1)/2} \int_{-\infty}^{\infty}\int_{-\infty}^{\infty} \exp\left(-\frac{ik}{z}uv\right) du\,dv \\ & \times \exp\left[-\frac{2u^2 + v^2/2 - 2(m+n)x_d u + (m-n)x_d v + (m^2+n^2)x_d^2}{w_0^2}\right] \exp\left[-\frac{v^2 + 2(m-n)x_d v + (m-n)^2 x_d^2}{2\sigma_0^2}\right] \\ & \times \exp\left\{-4\pi^2 k^2 z \int_0^1 \int_0^{\infty} \kappa \phi_n(\kappa,\alpha)\left[1 - J_0(\kappa\xi v)\right] d\kappa\, d\xi\right\} \delta''(v). \end{aligned} \tag{A.5}$$

Recalling the integral formulas $\int_{-\infty}^{\infty} \exp(-\beta^2 x^2 + \gamma x)\,dx = \sqrt{\pi}/\beta \exp[\gamma^2/(4\beta^2)]$ and $\int_{-\infty}^{\infty} f(x)\delta''(x)\,dx = f''(0)$, (A.3) can be rewritten as

$$\begin{aligned} F_1 = {} & \sqrt{\frac{\pi}{2}} w_0 \sum_{m=-(N-1)/2}^{(N-1)/2} \sum_{n=-(N-1)/2}^{(N-1)/2} \exp\left\{-\left(\frac{1}{2w_0^2} + \frac{1}{2\sigma_0^2}\right)(m-n)^2 x_d^2\right\} \\ & \times \left\{\left[w_0^2 + (m+n)^2 x_d^2\right] + \frac{4}{k^2}\left(\frac{1}{w_0^2} + \frac{1}{\sigma_0^2}\right)\left[1 - \left(\frac{1}{w_0^2} + \frac{1}{\sigma_0^2}\right)(m-n)^2 x_d^2\right] z^2 + \frac{8}{3}\pi^2 z^3 \int_0^{\infty} \kappa^3 \phi_n(\kappa,\alpha)\,d\kappa\right\}. \end{aligned} \tag{A.6}$$

Following the same procedure, (A.4) can be rewritten as

$$F_2 = \sqrt{\frac{\pi}{2}} w_0 \sum_{m=-(N-1)/2}^{(N-1)/2} \sum_{n=-(N-1)/2}^{(N-1)/2} \exp\left\{-\left(\frac{1}{2w_0^2} + \frac{1}{2\sigma_0^2}\right)(m-n)^2 x_d^2\right\}. \tag{A.7}$$

Upon substituting (A.6) and (A.7) into (A.2), (4) can be derived.

References

1. A. Zilberman, E. Golbraikh, N.S. Kopeika, Proc. SPIE **5160**, 397 (2004)
2. C. Rao, W. Jiang, N. Ling, Opt. Eng. **41**, 534 (2002)
3. D.T. Kyrazis, J.B. Wissler, D.D.B. Keating, A.J. Preble, K.P. Bishop, Proc. SPIE **2120**, 43 (1994)
4. A.S. Gurvich, M.S. Belen'kii, J. Opt. Soc. Am. A **12**, 2517 (1995)
5. A. Zilberman, E. Golbraikh, N.S. Kopeika, A. Virtser, I. Kupershmidt, Y. Shtemler, Atmos. Res. **88**, 66 (2008)
6. D. Dayton, B. Pierson, B. Spielbusch, J. Gonglewski, Opt. Lett. **17**, 1737 (1992)
7. M.S. Belen'kii, J.D. Barchers, S.J. Karis, C.L. Osmon, J.M. Brown II, R.Q. Fugate, Proc. SPIE **3762**, 396 (1999)
8. M.S. Belen'kii, S.J. Karis, C.L. Osmon, J.M. Brown, R.Q. Fugate, Proc. SPIE **3749**, 50 (1999)
9. L.J. Otten III, B.A. Jones, J. Lane, D.G. Black, M.C. Roggemann, Proc. SPIE **3866**, 23 (1999)
10. A. Zilberman, E. Golbraikh, N.S. Kopeika, Proc. SPIE **5987**, 598702 (2005)
11. R.R. Beland, Proc. SPIE **2375**, 6 (1995)
12. I. Toselli, L.C. Andrews, R.L. Phillips, V. Ferrero, Proc. SPIE **6708**, 670803 (2007)
13. I. Toselli, L.C. Andrews, R.L. Phillips, V. Ferrero, Opt. Eng. **47**, 026003 (2008)
14. X. Ji, B. Lü, Opt. Commun. **251**, 231 (2005)
15. G. Wu, H. Guo, S. Yu, B. Luo, Opt. Lett. **35**, 715 (2010)
16. X. Ji, X. Li, J. Opt. Soc. Am. A **26**, 236 (2009)
17. P. Zhou, Y. Ma, X. Wang, H. Zhao, Z. Liu, Opt. Lett. **35**, 1043 (2010)
18. X. Ji, P. Zhou, Appl. Phys. B **93**, 915 (2008)
19. I. Toselli, L.C. Andrews, R.L. Phillips, V. Ferrero, Proc. SPIE **6551**, 65510E (2007)